Direct evidence for a metallic interlayer band in Rb-intercalated bilayer graphene

J. Kleeman,[1] K. Sugawara,[2] T. Sato,[1] and T. Takahashi[1,2]
[1]*Department of Physics, Tohoku University, Sendai 980-8578, Japan*
[2]*WPI Advanced Institute for Materials Research, Tohoku University, Sendai 980-8577, Japan*
(Received 11 October 2012; revised manuscript received 1 March 2013; published 1 May 2013)

We have fabricated Rb-intercalated bilayer graphene on 6H-SiC(0001) and performed low-energy electron diffraction (LEED) and high-resolution angle-resolved photoemission spectroscopy (ARPES). In LEED experiments, we observed a 2×2 pattern identical to that of the bulk graphite intercalation compound C_8Rb. The existence of a 2×2 Rb layer is also confirmed by ARPES, where band folding due to the periodic potential of intercalated atoms was observed. All these results indicate that Rb atoms are intercalated between the two graphene monolayers in a regular manner similar to that of bulk C_8Rb. Further, we observed a parabolic metallic band at the Brillouin-zone center, analogous to the so-called interlayer band, which is thought to play an important role for the superconductivity in graphite intercalation compounds.

DOI: 10.1103/PhysRevB.87.195401 PACS number(s): 73.22.Pr, 79.60.Jv, 71.20.Tx, 74.25.Jb

I. INTRODUCTION

Graphite intercalation compounds (GICs) represent a large class of materials consisting of foreign atomic layers inserted between the weakly coupled carbon layers of bulk graphite.[1,2] Superconductivity has been recorded in a wide variety of GICs including alkali-metal compounds C_8K, C_8Rb, and C_8Cs.[1–5] Recently, the discovery of an unexpectedly high superconducting transition temperature in C_6Ca and C_6Yb[6] has revived the long-standing debate over the electronic structure and subsequent superconducting mechanism of GICs. Although it is generally accepted that charge transfer from the intercalated atoms triggers the superconductivity, the charge balance between the π^* band and the so-called interlayer band has remained controversial, as seen by the two distinctly different models for the electronic structure of GICs.[7,8] This difference is directly related to the character of electrons and phonons involved in the superconductivity. While a recent angle-resolved photoemission spectroscopy (ARPES) study[9] has reported the existence of the interlayer band below the Fermi level (E_F) at the Γ point in C_6Ca in line with the theoretical prediction,[10–12] the existence of the metallic interlayer band is still hotly debated.[13–17]

The interlayer electron is located just between two graphite layers in GICs and forms a free-electron-like electronic state with a parabolic dispersion. In this sense, metal-intercalated bilayer graphene may be regarded as the two-dimensional (2D) limit of GIC. Recently, the possibility of superconductivity in metal-deposited monolayer graphene has been proposed[18] and many attempts have been performed to fabricate metal (alkali metals and gold, etc.) adsorbed monolayer graphene.[19–23] However, superconductivity has not been reported yet. It is worth noting that a free-electron-like band corresponding to the GIC interlayer band has not been observed in these metal-deposited monolayer graphene samples. It is not clear at present whether the absence of superconductivity and the interlayer band in metal-deposited monolayer graphene is due to the disordered nature of deposited metals, in contrast to the regularly arranged intercalants in GICs, and/or the lack of an adjoining graphene sheet which sandwiches the metal atoms. In order to address this problem in metal-deposited monolayer graphene and the controversy in the charge balance between the π^* band and the interlayer band in bulk GICs, it is very important to fabricate a fully 2D GIC, namely metal-intercalated bilayer graphene, and clarify the electronic structure.

In this article, we report the fabrication of Rb-intercalated bilayer graphene on a SiC(0001) surface and its characterization by low-energy electron diffraction (LEED) and ARPES. We observed a clear 2×2 LEED pattern in Rb-deposited bilayer graphene similar to that of bulk C_8Rb, which indicates the regular arrangement of Rb atoms. ARPES results have revealed that the band dispersion is folded by the superstructure of the regularly intercalated Rb atoms. Further we clearly observed a free-electron-like metallic band at the Brillouin-zone (BZ) center. This indicates that the metallic interlayer band, which is thought to play a key role in driving the superconductivity,[7,10–12] is also present in the thinnest limit of GICs.

II. EXPERIMENTS

Bilayer graphene was prepared on a 6H-SiC(0001) single crystal by heating the crystal at temperature between 1500 and 1600 °C.[24] The crystal was kept in argon atmosphere of 1.1 MPa during the heating process to ensure large, flat terrace growth.[25] We verified by ARPES that the sample grown on the 6H-SiC(0001) crystal consists of unambiguously two graphene layers, with no mixing of mono- or trilayer graphene. The relatively large terrace size ($\sim$5 μm) was observed by atomic force microscopy. Intercalation of alkali atoms was achieved *in situ* by depositing Rb atoms on the bilayer graphene film from an alkali-atom dispenser (SAES getter) under ultrahigh vacuum of about 3×10^{-10} Torr. The sample was kept at 80–90 K during the deposition to promote the well-ordered intercalation.[26,27]

ARPES measurements were performed using a VG-SCIENTA SES-2002 spectrometer with a high-flux helium discharge lamp and a toroidal grating monochromator. The He IIα (40.814 eV) resonance line was used to excite photoelectrons. The energy and angular resolutions were set at 16 meV and 0.2° respectively. The temperature of the samples was maintained at 30 K during the ARPES measurements.

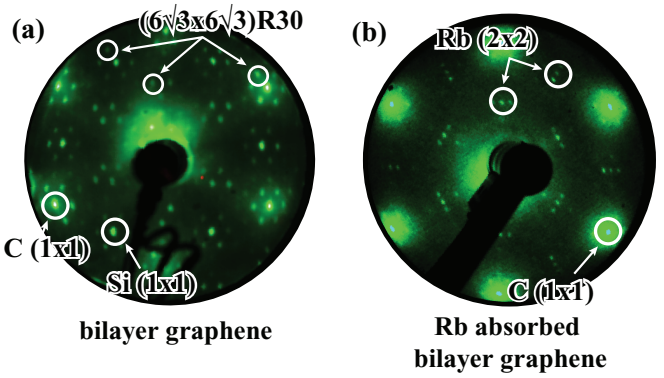

FIG. 1. (Color online) LEED patterns of (a) bilayer graphene and (b) Rb-deposited bilayer graphene grown on SiC, measured with a primary electron energy of 125 eV.

The Fermi level of samples was referred to that of a gold film deposited on the sample holder.

III. RESULTS AND DISCUSSION

Figure 1(a) shows the LEED pattern of bilayer graphene grown on SiC(0001). We observe the 1×1 SiC substrate pattern, the $6\sqrt{3} \times 6\sqrt{3}$ $R30^\circ$ spots from the buffer layer, and the 1×1 carbon lattice pattern in good agreement with previous reports.[24,25] After deposition of Rb atoms, a new structure with the 2×2 periodicity emerges as seen in Fig. 1(b). This indicates the formation of an ordered alkali-metal layer. The observed superstructure is analogous to that of bulk C_8Rb, although markedly different from the $\sqrt{3} \times \sqrt{3}$ $R30^\circ$ pattern of bulk C_6Li.[1] According to previous experiments of depositing Rb atoms onto graphite,[26,27] Rb atoms are readily intercalated into the surface of graphite above 80 K, forming a 2×2 monolayer under the topmost layer before diffusing into the bulk. It is inferred that the relatively large atomic size of Rb atom hinders them from penetrating rapidly into the graphite lattice.[1,28] In our experiments, a low-intensity highly dispersive LEED pattern was observed just after the deposition, which then gradually developed into a clear 2×2 pattern once the sample was heated slightly above 80 K. This indicates that Rb atoms deposited on bilayer graphene are readily intercalated between two graphene layers upon heating the sample as in the case of graphite surface.[26,27] In contrast, when we deposited Rb atoms on monolayer graphene, we did not observe a clear 2×2 superstructure even after heating the sample above 80 K. This supports the above conclusion that Rb atoms are actually intercalated bilayer graphene and form the well-ordered 2×2 superstructure.

Figures 2(a) and 2(b) show the valence-band dispersion measured along the ΓK direction of the graphene BZ for Rb-intercalated and pristine bilayer graphene, respectively. While the band structure of intercalated bilayer graphene is dominated by the prominent σ and π bands as in pristine bilayer graphene, the band dispersion is shifted toward higher binding energies by about 0.3 eV, suggesting a substantial electronic charge transfer from the alkali atoms to the graphene layers. Two strong nondispersive features at 15 and 16 eV in Rb-intercalated bilayer graphene are attributed to the Rb $4p$

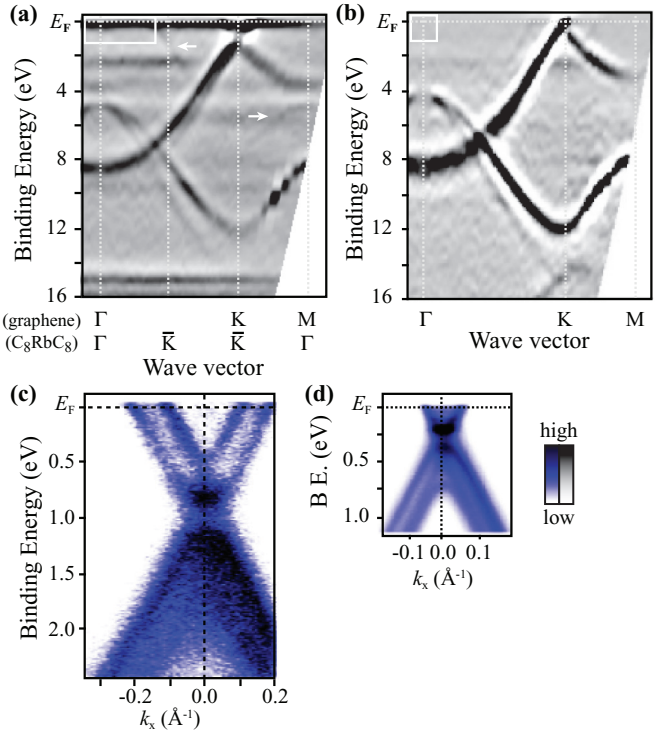

FIG. 2. (Color online) Experimental band dispersion of (a) Rb-intercalated and (b) pristine bilayer graphene (Ref. 24) obtained by taking the second derivative of ARPES spectral intensity as a function of wave vector and binding energy. White arrows indicate folded bands. White rectangles in (a) and (b) show the measured regions around Γ point shown in Figs. 4(b) and 4(c). Expansion of band structure near E_F around K point of (c) Rb-intercalated and (d) pristine bilayer graphene (Ref. 24).

core levels.[27,29] In addition to the prominent dispersive π and σ band and the flat Rb $4p$ core levels, we observed weak but highly dispersive bands around the midpoint between Γ and K [$\bar{K}$ point in Fig. 2(a)] in Rb-intercalated bilayer graphene. It is noted that these weak features are not observed in pristine bilayer graphene. These newly emerging bands are assigned to the folded π and σ bands due to the superstructure of intercalated atoms, as the band dispersion at the $\bar{K}$ point mirrors the π band at the K point while the dispersive band with its maximum around 5 eV at the M point is similar to the σ band at the Γ point.

Figures 2(c) and 2(d) show the expansion of the band dispersions near E_F around the K point for Rb-intercalated and pristine graphene, respectively. We at first notice that the intersection of the two almost straight bands (Dirac point) in pristine bilayer graphene grown on SiC is located at 0.33 eV in binding energy, and is shifted downward to 1.0 eV in Rb-intercalated bilayer graphene. While the initial shift of the Dirac point of 0.33 eV from E_F in pristine bilayer graphene is probably due to the charge transfer from the SiC substrate,[24] the additional downward shift to 1.0 eV is definitely due to the charge transfer from Rb atoms to graphene layers. We also find in Fig. 2(c) that a small band gap looks to open between the π and π^* bands in Rb-intercalated bilayer graphene, similar to various ARPES results on bulk GICs,[13–15,17,27]

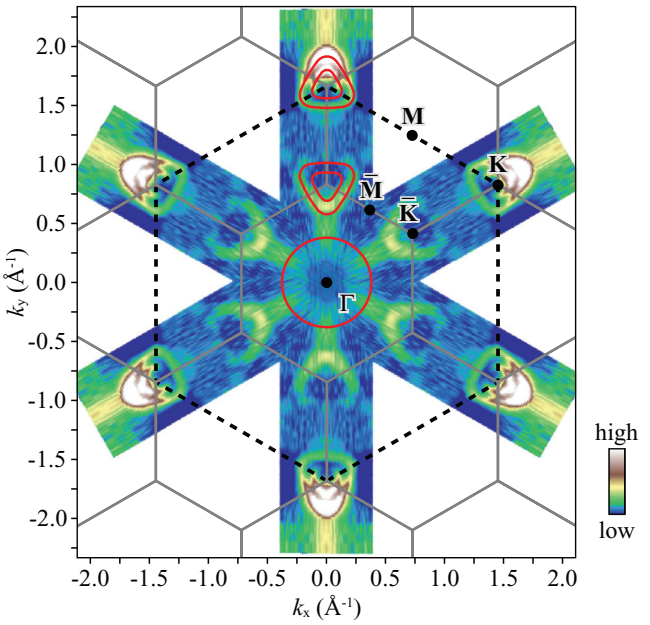

FIG. 3. (Color online) ARPES intensity at E_F of Rb-intercalated bilayer graphene plotted as a function of the 2D wave vector. Intensity at E_F is obtained by integrating the ARPES spectral intensity within ±30 meV with respect to E_F. Broken and solid black lines show the two-dimensional BZ of graphene and the 2 × 2 folded BZ, respectively. Red lines are guidelines for the k_F points.

but contrary to the band calculations.[7,8] According to recent theory[30,31] this gap opening may be related to the change in the distance between intercalated atoms and carbon atoms.

To elucidate the band-folding effect in intercalated bilayer graphene in more detail, we plot in Fig. 3 the ARPES intensity near E_F of Rb-intercalated bilayer graphene as a function of the 2D wave vector. The Fermi surface (FS) of Rb-intercalated bilayer graphene is significantly modified from that of pristine bilayer graphene, as demonstrated by a double-triangular contour at the K point. This newly emerging FS at the K point is attributed to the π^* band of graphene which is located above E_F in undoped graphene and is pulled down below E_F by charge transfer from the alkali atoms. We also find additional weak features around the $\bar{K}$ point in intercalated bilayer graphene, which resemble the FS at the K point of graphene BZ. This additional FS at the $\bar{K}$ point is a replica of the π^* band folded due to the 2 × 2 periodic potential of intercalated Rb atoms. In fact, the shape and volume of the additional FS is in good agreement with the FS at the K point.

Figures 4(a) and 4(b) show a set of near-E_F ARPES spectra and the intensity plot around the Γ point, respectively, for Rb-intercalated bilayer graphene, where we find a weak intensity variation showing a parabolic band dispersion symmetric with respect to the Γ point at E_F. Figures 4(c) and 4(d) show similar ARPES intensity plots for pristine and Li-intercalated bilayer graphene, respectively. In pristine bilayer graphene, we do not observe any band dispersions in this energy and momentum region as seen in Fig. 4(c). In Li-intercalated bilayer graphene [Fig. 4(d)], on the other hand, we observe two steep band dispersions symmetric with respect to the Γ point. These band are assigned to the folded π^* band since the $\sqrt{3} \times \sqrt{3}\ R30^\circ$ superstructure of intercalated Li atoms folds the original π^* band at the K point to the Γ point. It is noted here that there are no additional features near E_F around the Γ point. On the other hand, in Rb-intercalated bilayer graphene [Fig. 4(b)], we observe a relatively strong dispersive feature around $k_y = 0.65$ Å^{-1}, which is assigned to the folded π^* band at the $\bar{K}$ point of the 2 × 2 folded BZ. Since the superstructure is different between Li- and Rb-intercalated bilayer graphene ($\sqrt{3} \times \sqrt{3}\ R30^\circ$ vs 2 × 2), the original π^* band at the K point is folded to the Γ point in the Li case while it is folded to the $\bar{K}$ point just between the Γ and K points in the Rb case (see Fig. 3). This means that no replica of the π^* band should appear around the Γ point in Rb-intercalated bilayer graphene. Nevertheless, as seen in Fig. 4(b) we observe a faint but well symmetric band dispersion near E_F in Rb-intercalated bilayer graphene. We ascribe this band to the interlayer band, because, as discussed above, no replica of the π^* band appears at the Γ point and the shape and position of band dispersion are in good agreement with the theoretically predicted interlayer band.[10–12,31] The absence of a similar parabolic band in pristine and Li-intercalated bilayer graphene strengthens this conclusion.[7,10–12] The observed weak intensity of the parabolic band in Rb-intercalated bilayer graphene further confirms the above assignment because the interlayer state originating essentially from the Rb 5s state has a very small photoionization cross section (0.02 Mbarn) at the photon energy used in this experiment (40.8 eV), compared with those of the C 2s (1.9 Mbarn) and C 2p (1.2 Mbarn) states.[33]

Next, we estimate the electron occupancy in the π^* and the interlayer band from the volume of FS in Fig. 3. It is 0.40 ± 0.05 e^- and 0.53 ± 0.10 e^- for the π^* and the interlayer band, respectively. This indicates that the Rb atoms intercalated between the graphene layers are almost fully ionized and the donated electronic charges are transferred almost equally to the π^* and the interlayer band. This result is in good agreement with previous photoemission studies of bulk C_8Rb[14], suggesting that the distribution ratio of donated electrons between the π^* and the interlayer band may be similar in bilayer graphene and bulk graphite. It is noted here that the total electron count donated from Rb atoms is almost 1 e^- (0.40 + 0.53 e^-) per unit cell. This suggests that Rb atoms are intercalated with the well-ordered 2 × 2 superstructure between graphene layers, but do not reside on the surface or in the interface between graphene and SiC crystal.

The present observation of the interlayer band in Rb-intercalated bilayer graphene may shed light on the mechanism of superconductivity in bulk GICs. It has been intensively argued that a key to understanding the superconducting mechanism lies in the existence or absence of a metallic interlayer band at the Γ point.[7,10–12] The present ARPES study has revealed that the metallic interlayer band exists in Rb-intercalated bilayer graphene in contrast to Li-intercalated bilayer graphene. This closely resembles the case of three-dimensional GICs where C_8Rb is superconducting[5] while C_6Li is not.[1] Hence the present ARPES result not only provides evidence for an essential similarity of electronic states irrespective of the dimensionality, but also suggests a crucial

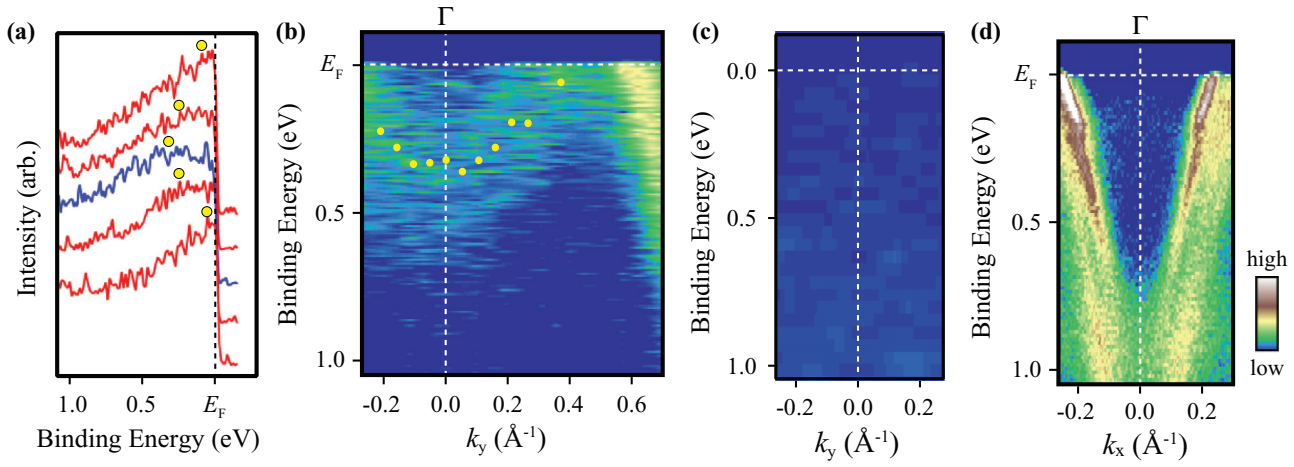

FIG. 4. (Color online) (a) and (b) A set of near-E_F ARPES spectra around Γ point for Rb-intercalated bilayer graphene and its intensity plot, respectively. Yellow dots in (a) and (b) show the peak position in ARPES spectrum determined by numerical fittings with Lorentzians. (c) and (d) Near-E_F ARPES-intensity plot for pristine and Li-intercalated bilayer graphene (Ref. 32), respectively. The measured regions for (b) and (c) are shown by white rectangles in Figs. 2(a) and 2(b).

role of the interlayer band as a mechanism of superconductivity in GICs.

IV. CONCLUSION

We have succeeded in fabricating Rb-intercalated bilayer graphene on SiC(0001). LEED and ARPES measurements have confirmed that Rb atoms are intercalated in a regular manner as in bulk C_8Rb, forming the 2×2 superstructure between graphene layers. The ARPES experiment has revealed that there is a metallic interlayer band at the center of the Brillouin zone in Rb-intercalated bilayer graphene in contrast to metal-deposited monolayer graphene. This suggests that the appearance of a metallic interlayer band is closely related to the GIC crystal structure, wherein metal atoms are sandwiched by two graphene sheets.

ACKNOWLEDGMENTS

We would like to thank K. Kanetani and Toru Takahashi for their help in the ARPES experiments. This work was supported by JSPS (KAKENHI 23224010 and 24740216).

[1]M. S. Dresselhaus and G. Dresselhaus, Adv. Phys. **51**, 139 (2002).
[2]T. Enoki, S. Miyajima, M. Sano, and H. Inokuchi, J. Mater. Res. **5**, 435 (1990).
[3]N. B. Hannay, T. H. Geballe, B. T. Matthias, K. Andres, P. Schmidt, and D. MacNair, Phys. Rev. Lett. **14**, 225 (1965).
[4]Y. Koike, H. Suematsu, K. Higuchi, and S. Tanuma, Physica B+C **99**, 503 (1980).
[5]M. Kobayashi, T. Enoki, H. Inokuchi, M. Sano, A. Sumiyama, Y. Oda, and H. Nagano, Synth. Met. **12**, 341 (1985).
[6]T. E. Weller, M. Ellerby, S. S. Saxena, R. P. Smith, and N. T. Skipper, Nat. Phys. **1**, 39 (2005).
[7]T. Ohno. K. Nakao, and H. Kamimura, J. Phys. Soc. Jpn. **47**, 1125 (1979).
[8]D. P. DiVincenzo and S. Rabii, Phys. Rev. B **25**, 4110 (1982).
[9]K. Sugawara, T. Sato, and T. Takahashi, Nat. Phys. **5**, 40 (2009).
[10]G. Csányi, P. B. Littlewood, A. H. Nevidomskyy, C. J. Pickard, and B. D. Simons, Nat. Phys. **1**, 42 (2005).
[11]M. Calandra and F. Mauri, Phys. Rev. Lett. **95**, 237002 (2005).
[12]I. I. Mazin, Phys. Rev. Lett. **95**, 227001 (2005).
[13]T. Takahashi, N. Gunasekara, T. Sagawa, and H. Suematsu, J. Phys. Soc. Jpn. **55**, 3498 (1986).
[14]N. Gunasekara, T. Takahashi, F. Maeda, T. Segawa, and H. Suematsu, Z. Phys. B **70**, 349 (1988).
[15]A. Grüneis, C. Attaccalite, A. Rubio, D. V. Vyalikh, S. L. Molodtsov, J. Fink, R. Follath, W. Eberhardt, B. Büchner, and T. Pichler, Phys. Rev. B **80**, 075431 (2009).
[16]T. Valla, J. Camacho, Z.-H. Pan, A. V. Fedorov, A. C. Walters, C. A. Howard, and M. Ellerby, Phys. Rev. Lett. **102**, 107007 (2009).
[17]Z.-H. Pan, J. Camacho, M. H. Upton, A. V. Fedorov, C. A. Howard, M. Ellerby, and T. Valla, Phys. Rev. Lett. **106**, 187002 (2011).
[18]G. Profeta, M. Calandra, and F. Mauri, Nat. Phys. **8**, 131 (2012).
[19]A. Bostwick, T. Ohta, T. Seyller, K. Horn, and E. Rotenberg, Nat. Phys. **3**, 36 (2007).
[20]C. Virojanadara, S. Watcharinyanon, A. A. Zakharov, and L. I. Johansson, Phys. Rev. B **82**, 205402 (2010).
[21]S. Watcharinyanon, C. Virojanadara, and L. I. Johansson, Surf. Sci. **605**, 1918 (2011).
[22]J. L. McChesney, A. Bostwick, T. Ohta, T. Seyller, K. Horn, J. González, and E. Rotenberg, Phys. Rev. Lett. **104**, 136803 (2010).
[23]A. Varykhalov, J. Sánchez-Barriga, A. M. Shikin, C. Biswas, E. Vescovo, A. Rybkin, D. Marchenko, and O. Rader, Phys. Rev. Lett. **101**, 157601 (2008).
[24]K. Sugawara, T. Sato, K. Kanetani, and T. Takahashi, J. Phys. Soc. Jpn. **80**, 024705 (2011).
[25]K. V. Emtsev, A. Bostwick, K. Horn, J. Jobst, G. L. Kellogg, L. Ley, J. L. McChesney, T. Ohta, S. A. Reshanov, J. Röhrl, E. Rotenberg,

A. K. Schmid, D. Waldmann, H. B. Weber, and T. Seyller, Nat. Mater. **8**, 203 (2009).

[26]M. Caragiu and S. Finberg, J. Phys: Condens. Matter **17**, R995 (2005).

[27]J. Algdal, T. Balasubramanian, M. Breitholtz, T. Kihlgren, and L. Walldén, Surf. Sci. **601**, 1167 (2007).

[28]K. T. Chan, J. B. Neaton, and M. L. Cohen, Phys. Rev. B **77**, 235430 (2008).

[29]S. Hüfner, *Photoelectron Spectroscopy: Principles and Applications*, Springer Series in Solid-State Sciences, edited by H.-J. Cardona, Manuel Fulde, Peter Klitzing, and Klaus Von Queisser, Vol. 82, 2nd ed. (Springer, Saarbrucken, Germany 1996).

[30]T. P. Kaloni, Y. C. Cheng, M. Upadhyay Kahaly, and U. Schwingenschlögl, Chem. Phys. Lett. **534**, 29 (2012).

[31]T. P. Kaloni, M. Upadhyay Kahaly, Y. C. Cheng, and U. Schwingenschlögl, Europhys. Lett. **98**, 67003 (2012).

[32]K. Sugawara, K. Kanetani, T. Sato, and T. Takahashi, AIP Advances **1**, 022103 (2011).

[33]J. J. Yeh, *Atomic Calculation of Photoionization Cross Sections and Asymmetry Parameters* (Gordon and Breach Science Publishers, Langhorne, PA, 1993).